Journal of Saudi Chemical Society (2015) **19**, 147–154

King Saud University

Journal of Saudi Chemical Society

www.ksu.edu.sa
www.sciencedirect.com

ORIGINAL ARTICLE

The cellular response of *Saccharomyces cerevisiae* to multi-walled carbon nanotubes (MWCNTs)

Chantelle L. Phillips [a], Clarence S. Yah [a,d], Sunny E. Iyuke [a,*], Karl Rumbold [b], Viness Pillay [c]

[a] *School of Chemical and Metallurgical Engineering, University of the Witwatersrand, Johannesburg, P/Bag 3, Wits 2050, Gauteng, South Africa*
[b] *School of Molecular & Cell Biology, University of the Witwatersrand, Johannesburg, P/Bag 3, Wits 2050, South Africa*
[c] *Department of Pharmacy and Pharmacology, University of the Witwatersrand, 7 York Road, Parktown, 2193 Johannesburg, Gauteng, South Africa*
[d] *Biochemistry and Toxicology Section, National Institute for Occupational Health (NIOH), 25 Hospital Road, Constitutional Hill, Johannesburg, Gauteng, South Africa*

Received 11 November 2011; accepted 7 January 2012
Available online 14 January 2012

KEYWORDS

Saccharomyces;
Carbon Nanotubes;
Uptake;
Cellular response;
Toxicity

Abstract Nanoparticles (NPs) especially those of carbon nanotubes (CNTs) have remarkable properties that are very desirable in various biological and biomedical applications. This has necessitated the rapid study of CNT toxicities, to augment their safe use, particularly, in yeast cells. The yeast cell; *Saccharomyces cerevisiae* is a widely used industrial and biological organism with very limited data regarding their cellular behaviour in NPs. The current study examines the cellular response of *S. cerevisiae* to MWCNTs. The CNTs were produced by the swirled floating catalytic chemical vapour deposition (SFCCVD) method and covalently functionalised using 1,3-dipolar cycloaddition. The CNT properties such as size, surface area, quality and surface vibrations were characterized using TEM, SEM, BET, TGA and Raman spectroscopy, respectively. The cellular uptake was confirmed with a *FITC* functionalised MWCNTs using 1H NMR, SEM and TEM. The CNT concentrations of 2–40 μg/ml were used to determine the cellular response through cell growth phases and cell viability characteristics. The TEM and SEM analyses showed the production of MWCNTs with an average diameter of 53 ± 12 nm and a length of 2.5 ± 0.5 μm. The cellular uptake of *FITC*-MWCNTs showed 100% internalisation in the yeast cells. The growth

* Corresponding author. Tel.: +27 11 717 7546; fax: +27 86 553 6435.
E-mail address: sunny.iyuke@wits.ac.za (S.E. Iyuke).
Peer review under responsibility of King Saud University.

Production and hosting by Elsevier

http://dx.doi.org/10.1016/j.jscs.2012.01.005

curve responses to the MWCNT doses showed no significant differences at $P > 0.05$ on the growth rate and viability of the *S. cerevisiae* cells.

1. Introduction

Carbon nanotubes (CNTs) are molecular-scaled tubes of NPs known to possess tremendous mechanical, magnetic, and electrical properties, high flexibility, elasticity and low thermal expansion coefficient properties due to their unique topology and structure (Simate et al., 2010; Yah et al., 2011a,b). This has necessitated their noticeable interest in biomedical applications such as drug delivery (Bianco et al., 2005; Ngoy et al., 2011), medical imaging and cancer treatment (Shvedova et al., 2009; Wu et al., 2010). Due to increased carbon nanomaterials demand, production and applications; their interactions in the environment is inevitable. Furthermore, toxicological information on carbon-containing materials with environmental organisms is limited and published data on the toxic effects are contradictory (Warheit et al., 2004; Cheng et al., 2009). Some studies have indicated that NPs stimulate cells growth (Mitchell et al., 2004) while others, have shown an increase in cell death (Ghafari et al., 2008; Cheng et al., 2009). Yeast cell, *Saccharomyces cerevisiae* which is widely used in industrial and biological processes (Mitchell et al., 2004; Kasemets et al., 2009) have very limited data regarding their cellular behaviour to NPs. Furthermore, this species share major metabolic pathways and orthologies with humans and have the advantages of a well-studied model organism (Grossetête et al., 2010). Therefore, the use of yeast cell viability and the response effect to study the toxicity of CNT will provide an excellent tool for determining a prototype similar to humans. Currently, there are very limited data on the viability and cellular response effects to NPs using yeast cells as a model. The current study therefore, aimed to investigate the viability and cellular response of preteine CNTs (p-CNTs) and functionalised CNTs (f-CNTs) of *S. cerevisiae in vitro*. The use of f- CNTs are essential for the integration of these materials into different systems for technological, biological and biomedical applications (Pastorin et al., 2006).

2. Materials and methods

Ferocene, sulphuric and nitric acid, methanol, diethyl ether, ethanol, sodium sulphate anhydrous, acetone, D-glucose powder, polyethyleneimine, peptone buffered water, sodium carbonate anhydrous, glycerol, malt extract agar , peptone powder and yeast extract powder were obtained from Merck Chemicals (Pty) Ltd., South Africa. Thionyl chloride, paraformaldehyde, *N*-ethyldi-isopropulamine and ninhydrin were obtained from Merck, Schuchardt OHG,Honenbrum, Germany. Chloroform-d, red cell linker kit, fluorescein isothiocyanate (FITC) and *N*-tritylglycine 98% were obtained from Sigma–Aldrich, Steinheim, Germany and 90 mm petri-dishes from Plastpro Scientific, Edenvale, Gauteng, SA. All the regents and chemicals used in the study were of analytical grade.

2.1. The production and functionalisation of carbon nanotubes

The modification of chemical vapour deposition (CVD), termed as the swirled floating catalyst (SFCCVD) was used to produce the MWCNTs according to Yah et al. (2011b). The *p*-MWCNTs were functionalised using purified H_2SO_4/HNO_3 in a 3:1 (v/v) ratio and 30% HNO_3 acid to create carboxylic groups (–COOH) by sonication for further coupling (Ngoy et al., 2011). The oxidised MWCNTs (*o*-MWCNTs) were coupled with thionyl chloride to create the negative charge necessary for amide coupling. The 1,3-dipolar cycloaddition coupling of *N*-tritylglycine, the deprotection of the trityl group from the protected MWCNTs-COCl glycine and the coupling of fluorescent probe on MWCNT-free amide sites were done according to Georgakilas et al. (2002) as shown in Fig. 1. The produced CNTs were characterised using TEM, BET, Raman spectroscopy, TGA and ^{1}H NMR. The various MWCNTs were then sterilely (filtration) and serially (10 fold dilution) diluted in a biosafety cabinet and sonicated as stock for further analyses.

2.2. Cultivation of S. cerevisiae

The pure *S. cerevisiae* strain used throughout the work was obtained from the School of Molecular and Cell Biology of the University of the Witwatersrand and maintained onto malt extract agar (MEA) for further use. The growth curves of the *S cerevisiae* inoculated with pristine and *f*-MWCNTs: 2, 3, 6, 10, 20 and 40 μg/ml were monitored on peptone and glucose (YPD) by measuring the absorbance of light by the yeast sample using a spectrophotometer (Ultrospec 2000 UV–vis spectrophotometer). The cell viability was determined using the standard plate count. The cell imaging of *S. cerevisiae* was done using *the* linker kit (PKH26-GL) according to the manufacturer's instructions. The cells were then viewed with a Zeiss confocal laser fluorescence scanning microscope.

3. Results and discussion

3.1. Transmission electron microscopy (TEM) analysis

The TEM micrographs of *p*-MWCNTs are shown in Fig. 2a while the acids *o*-MWCNTs (1:3 HNO_3/H_2SO_4 acid and nitric acid) are shown in Fig. 2b and c. The MWCNTs structures' ranged from 53 ± 12 nm in diameter and lengths of 2.5 ± 0.5 μm. The results are similar those earlier reported by Abdulkareem et al. (2007) and Yah et al. (2011b). The SEM images of the pristine and *o*-MWCNTS are shown in Fig. 3a–c with length distribution of 1 ± 0.5 μm.

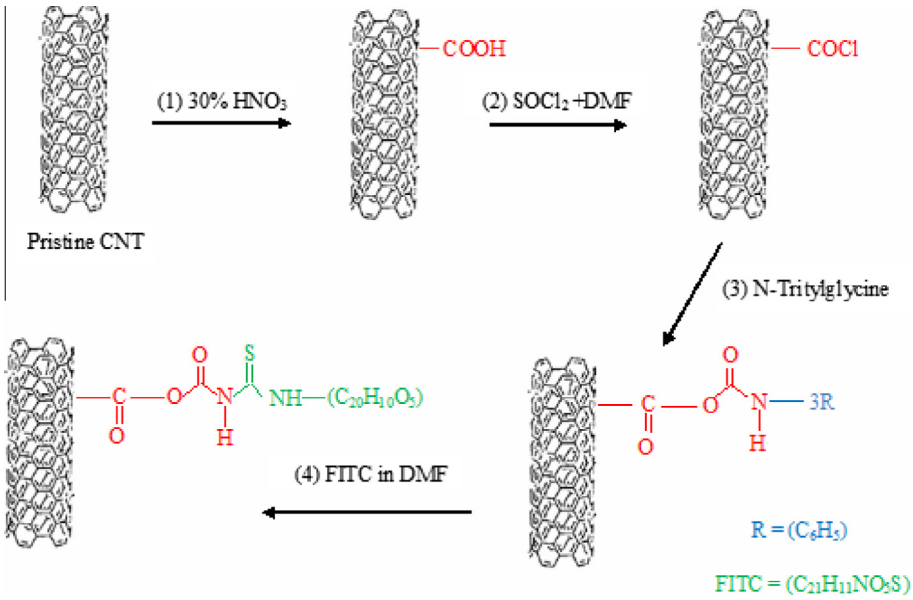

Figure 1 Schematic reaction of 1,3-dipolar cycloaddition of tritylglycine protected and functionalisation of the MWCNT.

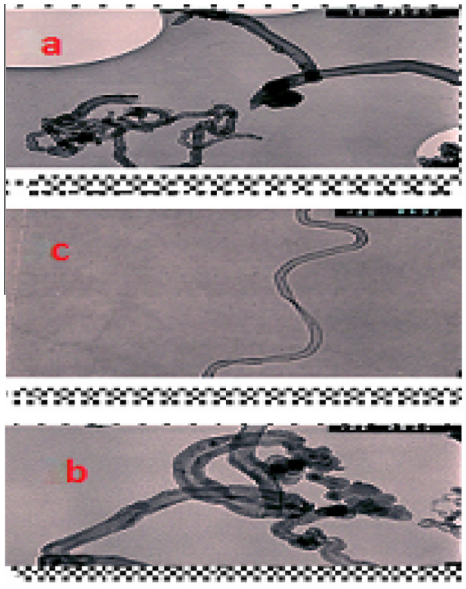

Figure 2 (a) TEM micrograph of pristine MWCNTs, (b) oxidised MWCNTs after 1:3 HNO_3/H_2SO_4 acid treatment and (c) 30% HNO_3 oxidized MWCNTs.

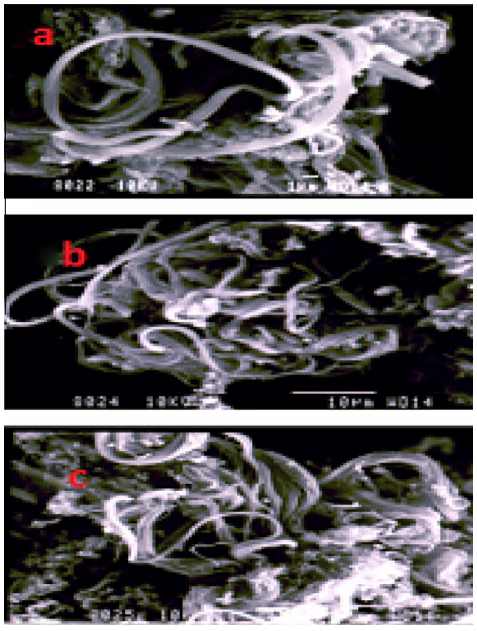

Figure 3 (a) SEM Micrograph of *p*-MWCNTs, (b) 30% HNO_3 oxidized and (c) 1:3 HNO_3/H_2SO_4 oxidised MWCNTs.

3.2. The Brunauer–Emmett–Teller (BET) analysis of the MWCNT

The BET results in Table 1 show the surface area (SA), average pore volume and average pore diameter of pristine, 30% HNO_3 acid and 1:3 HNO_3/H_2SO_4 acid treated MWCNTs, respectively. There was no significant difference between the surface area of the untreated and treated MWCNTS. The surface area was not as large as those reported by Bacsa et al. (2000).

3.3. The Raman spectroscopy analysis of the MWCNT

The Raman spectra of pristine, 30% HNO_3 and 1:3 HNO_3/H_2SO_4 treated MWCNTs at 514.5 nm are shown in Table 2. The spectra of the D bands correspond to disordered carbon around 1350 cm^{-1} while the G bands and the split tangential mode occurred around 1500–1600 cm^{-1}. The Raman spectra differed from those reported by Bacsa et al. (2000) and Yah et al. (2011a) that had a higher proportion of tubular carbon. The closer the ID/IG to 1 the better the quality of CNTs produced. Nitric acid treated CNTs (ID/IG = 1.01) produced the

Table 1 BET results of MWCNTs.

Sample	SA (m^2/g)	Average pore volume (cm^3/g)	Average pore diameter (nm)
Pristine MWCNTs	31.6	0.16	20.6
30% HNO_3 treated MWCNTs	36.0	0.16	17.3
1:3 HNO_3/H_2SO_4	29.5	0.10	13.4

Table 2 Raman spectra results of pristine, 30% HNO_3 and 1:3 HNO_3/H_2SO_4 MWCNTs treated.

Sample	Band position		Band intensity		Intensity ratio ID/IG	Band width	
	D1	G	ID	IG		D1	G
Pristine MWCNTs	1324	1587	37	36	1.03	194	75
30% HNO_3 acid treated MWCNTs	1321	1584	72	71	1.01	182	74
1:3 HNO_3/H_2SO_4 acid treated MWCNTs	1327	1582	36	26	1.39	159	97

best MWCNTs that can be used for further application as opposed to pristine and nitric/sulphuric acid MWCNTs.

From the TGA analysis, the *p*-MWCNTs were found to decompose easily and reported the highest value of the metal catalyst (13.20%). 30% HNO_3 oxidation showed 9.70% while 1:3 HNO_3/H_2SO_4 reported catalyst impurities of 11.67%. Thus the 30% HNO_3 treatment removed more metal catalysts than 1:3 HNO_3/H_2SO_4 (data not shown). The thermal stability of CNTs depends on the side wall "defects" and the amount of metallic impurities. The thermal properties of the MWCNTs from the 1,3-dipolar cycloaddition reaction were investigated by TGA. The residual amount of impurities in the functionalised sample was 0.5% in comparison to the non-functionalised MWCNTs with residual impurities of 10.5% (data not shown).

3.4. Characterisation of functionalised multiwalled carbon nanotubes

The carboxylic groups were introduced onto the surfaces of MWCNTs by employing acid treatment. The FITC was covalently attached to the *o*-MWNT via a 1,3-dipolar cycloaddition reaction of trityl protected glycine (Georgakilas et al., 2002). The progress of functionalisation was tracked by TEM, ^{1}H NMR spectroscopy, TGA and confocal microscopies.

TEM was used to investigate the structures of the un-functionalised product from the 1,3-dipolar cycloaddition reaction, *N*-tritylglycine functionalised MWCNTs and *FITC*-MWCNTs. Fig. 4a and b show the micrographs of *N*-tritylglycine functionalised MWCNTs and *FITC*-MWCNTs, respectively.

The ^{1}H NMR spectrum of *N*-tritylglycine functionalised MWCNTs shows the presence of the trityl chain at about 7.4 ppm as a broad peak, confirming the attachment of the trityl group.

Comparison of the ^{1}H NMR spectra of the protected and deprotected CNTs clearly show the presence or attachment of the trityl group as a broad peak at 7.4 ppm (data not shown) while the signal consequently disappeared after treatment with 4 M HCl in dioxane (data not shown).

3.5. Growth response of S. cerevisiae to MWCNTs

To test for the toxicity of CNTs we assessed the growth of the yeast species which were continuously exposed to disperse pristine and *o*-MWCNTs. Fig. 5 compares the growth curves of *S. cerevisiae* incubated with increasing concentrations of MWCNTs (2, 3, 5, 6, 10, 20 and 40 μg/ml) to the control (grown in the absence of *p*-MWCNTS) at lag, log and stationary phases. The results showed no significant differences between the growth curves in the exponential and stationary phases ($p > 0.05$). These results were similar to those reported by Kasemets et al. (2009) who used both nano and bulk TiO_2 to test the toxicity of yeast cells. Both the bulk and nano TiO_2 at EC_{50} values of > 200000 mg TiO_2/l caused no toxic response which was similar to earlier reports by Heinlaan et al. (2008) on bacteria *V. fisheri* (EC_{50} > 200000 mg/l). However, bulk and nano ZnO at a concentration of 250 mg/l was found to inhibit the growth of yeast profiles which were comparable to the toxicities of algae and *Vibrio fischeri* at concentrations of 0.034 and 0.030 ZnO mg/l and 1.8–1.9 mg of nano and bulk ZnO/l for bacteria (Heinlaan et al., 2008; Aruoja et al., 2009). The surface properties (large surface area) of MWCNTs are essential for the interactions of the yeast cell walls that constitute a prime site for the particles entry into the cells (Navarro et al., 2008).

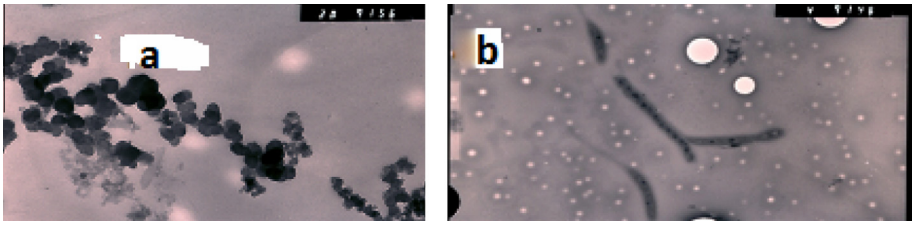

Figure 4 (a) TEM image of *N*-tritylglycine functionalised MWCNTs and (b) micrograph of *FITC*-MWCNT.

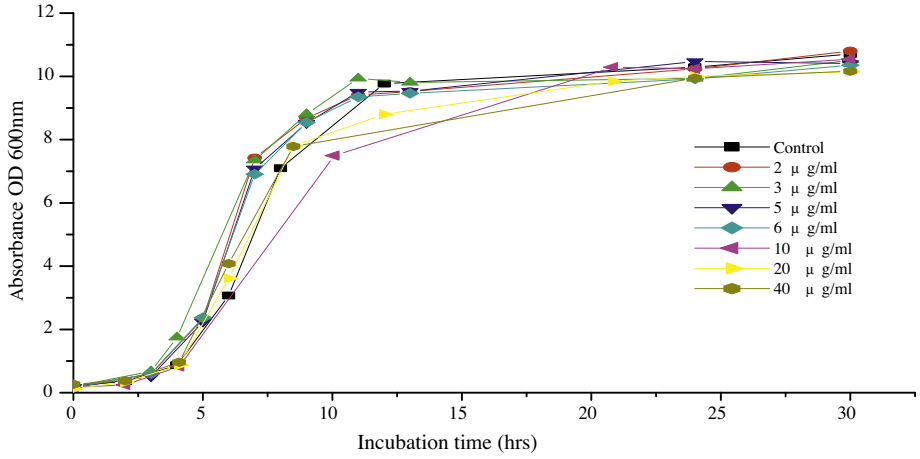

Figure 5 The growth response curve of *S. cerevisiae* incubated with different concentrations of *p*-MWCNTs to the control (incubated with no MWCNTs).

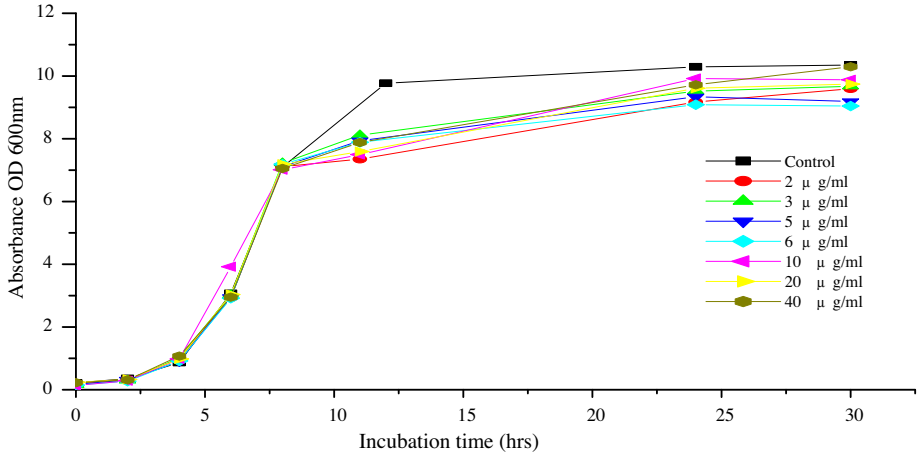

Figure 6 The growth response curve of *S. cerevisiae* incubated with different concentrations of oxidized MWCNTs to the control (incubated with no MWCNTs).

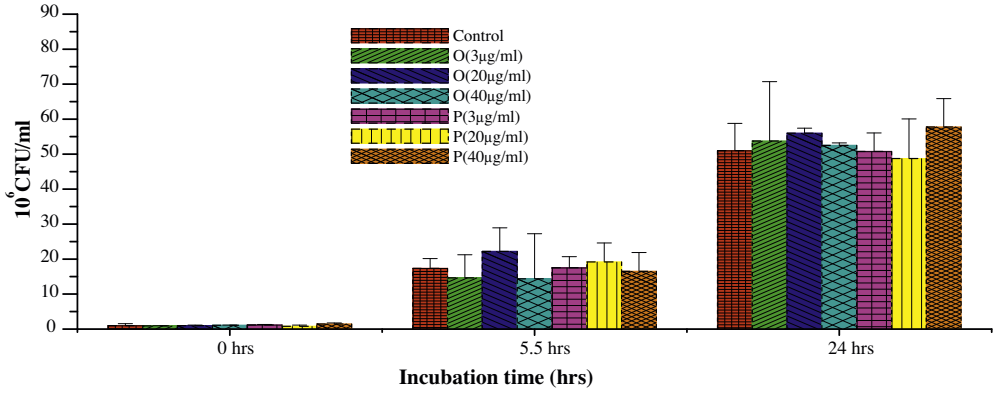

Figure 7 The cell viability response of *S. cerevisiae* incubated with different concentrations of pristine (P) and oxidized (O) MWCNTs to the control (C, without MWCNTs).

The result of the *o*-MWCNTs with the growth of *S. cerevisiae* cells are shown in Fig. 6. The results showed no response effect as compared to the control ($p > 0.05$) with no inherent cytotoxicity.

3.6. Cell viability of *S. cerevisiae* to MWCNTs

The cells were cultured on MEA and inoculated with both pristine and *o*-MWCNTs. Neither *p*-MWCNTs nor *o*-MWCNTs affected the viability at 30 °C on MEA plates as shown in Fig. 7. The results were similar to those earlier reported by Mitchell et al. (2004) who used gold and silver colloids to test for *Saccharomyces* toxicity. There was no significant difference between the cell viabilities of *p*-MWCNT and *f*-MWCBNT ($p > 0.05$).

3.7. Scanning electron microscopy analysis of *S. cerevisiae*

In order to elucidate the effect of CNTs on cell morphology, yeast cell suspensions were incubated with varying concentrations of CNTs and compared to the control which was incubated without CNTs. Yeast cells were incubated (concentrations 0, 25, 5 and 100 μg/ml of CNTs) for a period of 3 days. Fig. 8a–d show the morphological effect of the yeast cells to CNTs. The yeast cells in Fig. 8a and b were used as the control as compared to the treated cells in Fig. 8c and d.

After 3 days of incubation, *S. cerevisiae* cell suspensions showed no morphological damage at concentrations of 0, 25, 50 μg/ml of CNTs. However, the 100 μg/ml concentration of CNTs to *S. cerevisiae* cells showed a partial loss of content with a middle wall deformation as shown in Fig. 8c. Cells lost their intracellular content, resulting in an empty deformed cell wall. This suggests that at high concentrations CNTs may be toxic to cells. These results were similar to those reported by Adams et al. (2006) that at higher values TiO_2 inhibits the growth of *Bacillus subtilis* and *Escherichia coli* which was in line with those of Aruoja et al. (2009) that both bulk and nano TiO_2 can cause toxicity to microalgal cells. Close contact therefore between the MWCNTs and the yeast cells mostly has taken place before cell membrane deformation, disruption and leakage occurs. The disruption of the cell membranes can cause additional toxic effects such as reactive oxygen species (ROS) which mediate oxidative stress (Xu et al., 2011). The disruption of environmental organisms cell membranes leading to inflammation and oxidative stress from ROS damage (cellular proteins, DNA, lipids and carbohydrates) has been reported by Kasemets et al. (2009).

3.8. Fluorescein isothiocyanate (FTIC) confocal microscopy results

Fluorescence microscopy was used to track the distribution of MWCNT-*FITC* inside the cells. Confocal images clearly show

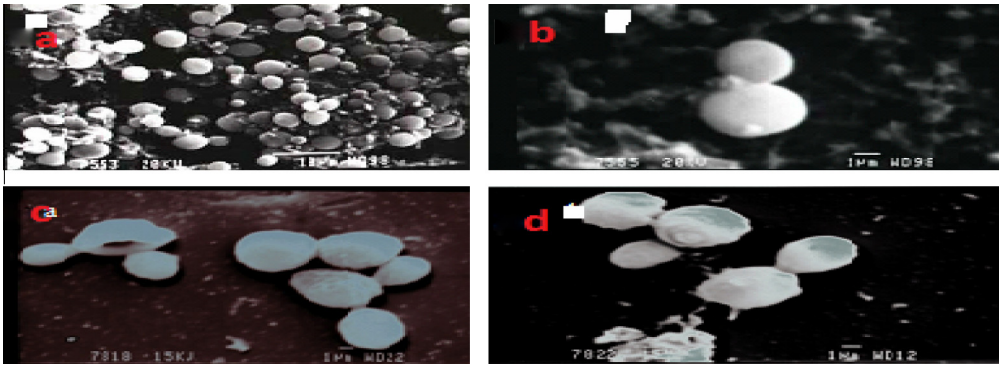

Figure 8 (a) SEM micrographs of *S. cerevisiae* incubated without MWCNTs, (b) illustrating a single budding *S. cerevisiae* cell, (c) micrographs of *S. cerevisiae* incubated with *p*-MWCNTs showing a single cell with loss of intracellular content and (d) group of *S. cerevisiae* cells with intact cell walls.

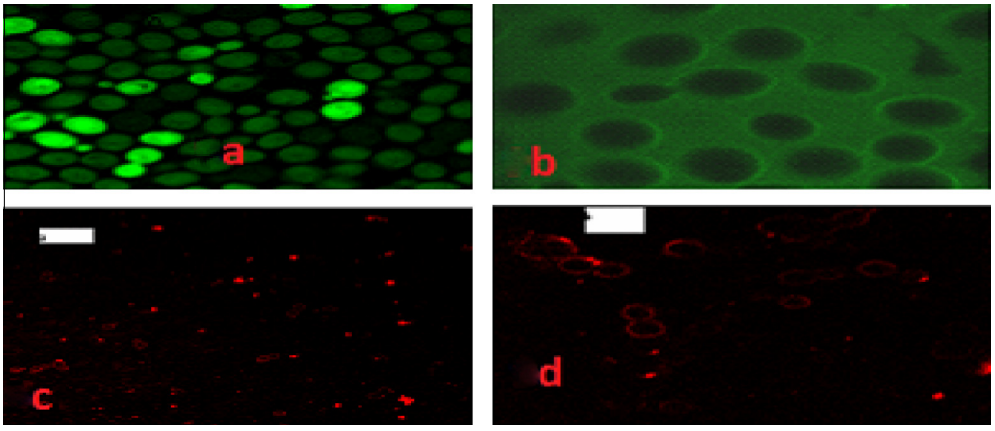

Figure 9 (a) Confocal image of *S. cerevisiae* cells incubated with MWCNT-*FITC*, (b) confocal image of *S. cerevisiae* cells incubated with *FITC*, (c and d) confocal images of red stained membrane of *S. cerevisiae* cells.

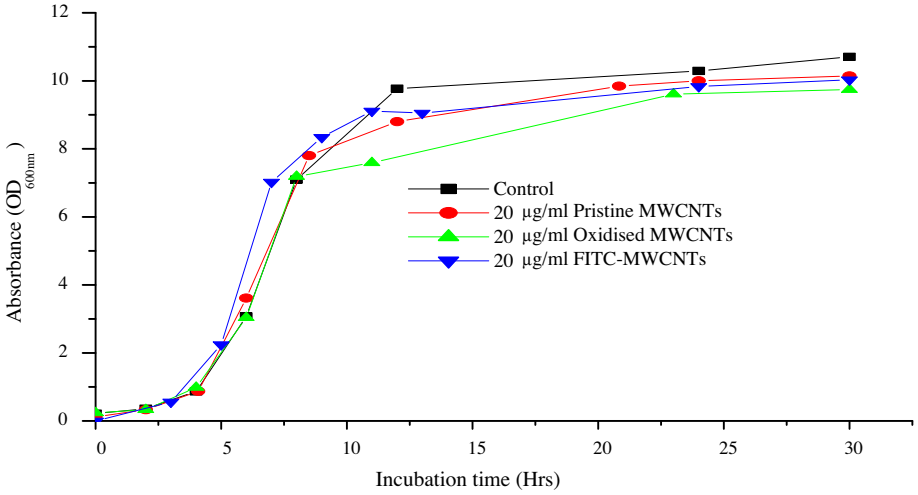

Figure 10 Growth response curve of *S. cerevisiae* incubated with 20 µg/ml pristine, oxidized, *FITC*-MWCNTs and the control.

that MWCNT-*FITC* is internalised by the yeast cells. After incubating the yeast cells with 20 µg/mL of *FITC*-MWCNT for 1 h green fluorescence was observed throughout the cell (Fig. 9a. Work done previously on different human cell types reported fluorescence FITC functionalised single walled carbon nanotubes (SWCNTs) concentrated at certain compartments of the cell such as the cytoplasm and nuclei without being toxic to the cell upto 10 µM (Pantarotto et al., 2004). The results were in agreement with those of Zhou et al. (2010) who showed that *FITC*-SWCNTs incubated with HeLa cells did not remain on the outside membrane but transversed the membranes and localised in the subcellular cell compartments of the lines. The results were dissimilar to the findings of Kostarelos et al. (2007) who reported CNT uptake by the cell at 60%. The present study, showed a huge uptake of the MWCNTs within the yeast cells. Cells incubated with *FITC* only (not conjugated to MWCNTs), showed no fluorescence within the cell and were restricted from across the cell membrane barrier (Fig. 9b). In order to examine *S. cerevisiae* cells incubated without MWCNTs by fluorescence microscopy, cells were stained with PKH 26GL Red fluorescent cell linker kit and examined under fluorescence microscopy. Fig. 9d and c show the red fluorescence cell membrane of the cells as well as the characteristic budding of yeast cells without signs of the CNTs internalisation. The results were in agreement with those of Zhou et al. (2010) who showed that *FITC* alone when incubated with HeLa cells remained on the outside membrane.

The influences of pristine and 30% nitric acid *o*-MWCNTs and *FITC*-MWCNTs on cell growth were assessed spectrophotometrically. The growth curves of pristine, *o*-MWCNTs and *FITC*-MWCNTs were compared to the control. The results showed no significant differences at $p > 0.05$ after 20 µg/ml of MWCNT incubation (Fig. 10). The *FITC*-MWCNTs uptake by *S. cerevisiae* cells, was similar in pattern to the control, pristine and *o*-MWCNTs.

4. Conclusion

The MWCNTs were produced by the SCCVD technique. The quality of purified MWCNTs resulting from the 30% HNO_3 was higher than that of 1:3 acid treated HNO_3/H_2SO_4. At both low (2 µg/ml) and high (40 µg/ml) concentrations of MWCNTs incubation, yeast cells induced no growth response and cell viability effect when compared to the control. However, higher concentrations of (100 µg/ml) MWCNTs may induce toxic effects. Un-conjugated *FITC* to MWCNTs was restricted from crossing the cell membrane barrier. The *FITC*-MWCNTs conjugates translocated inside all the cell compartments of the *S. cerevisiae*. The *FITC*-MWCNTs did not induce changes in the *S. cerevisiae* growth response. However, further experiments are needed to ascertain the toxicity because of its prime importance in biological and industrial applications.

Conflict of interest statement

None declared.

Acknowledgements

The authors are grateful for the financial support from the National Research Foundation (NRF) of South Africa and NRF Focus Area, Nanotechnology flagship programme, DST/NRF Centre of Excellence. The student bursaries provided by the Wits University and IBD/FoodBev Seta are much appreciated.

References

Abdulkareem, A.S., Afolabi, A.S., Iyuke, S.E., Pienaar, H.C., 2007. Synthesis of carbon nanotubes by swirled floating catalyst chemical vapour deposition method. Journal of Nanoscience and Nanotechnology 7 (9), 3233–3238.

Adams, L.K., Lyon, D.Y., Alvarez, P.J.J., 2006. Comparative ecotoxicity of nanoscale TiO_2, SiO_2 and ZnO water suspensions. Water Resources 40, 3527–3532.

Aruoja, V., Dubourguier, H.C., Kasemets, K., Kahru, A., 2009. Toxicity of nanoparticles of CuO, ZnO and TiO_2 to microalgae Pseudokirchneriella subcapitata. Science of the Total Environment 407, 1461–1468.

Bacsa, R.R., Laurent, C., Peigney, A., Bacsa, W.S., Vaugien, T., Rousset, 2000. High surface area carbon nanotubes from catalytic chemical vapor deposition process. Chemical Physics Letters 323 (5-6), 566–571.

Bianco, A., Kostarelos, K., Prato, M., 2005. Applications of carbon nanotubes in drug delivery. Current Opinion in Chemical Biology 9 (6), 674–679.

Cheng, C., Müller, K.H., Koziol, K.K.K., Skepper, J.N., Midgley, P.A., Welland, M.E., Porter, A.E., 2009. Toxicity and imaging of multi-walled carbon nanotubes in human macrophage cells. Biomaterials 30 (25), 4152–4160.

Georgakilas, V., Tagmatarchis, N., Pantarotto, D., Bianco, A., Briand, J.P., Prato, M., 2002. Amino acid functionalisation of water soluble carbon nanotubes. Chemical Communications 24, 3050–3051 (Cambridge, England).

Ghafari, P., St-Denis, C.H., Power, M.E., Jin, X., Tsou, V., Mandal, H.S., Bols, N.C., Tang, X.S., 2008. Impact of carbon nanotubes on the ingestion and digestion of bacteria by ciliated protozoa. Nature Nanotechnology 3 (6), 347–351.

Grossetête, S., Labedan, B., Lespinet, O., 2010. FUNGIpath: a tool to assess fungal metabolic pathways predicted by orthology. BMC Genomics 2010 (11), 81.

Heinlaan, H., IvasK, A., Blinova, I., Dubourguier, H.C., Kahru, A., 2008. Toxicity of nanosized and bulk ZnO, CuO and TiO_2 to bacteria *Vibrio fischeri* and crustaceans *Daphnia magna* and *Thamnocephalus paltyurus*. Chemosphere 71, 1308–1316.

Kasemets, K., Ivask, A., Dubourguier, H.-C., Kahru, A., 2009. Toxicity of nanoparticles of ZnO, CuO and TiO_2 to yeast *Saccharomyces cerevisiae*. Toxicity in Vitro 23, 1116–1122.

Kostarelos, K., Lacerda, L., Pastorin, G., Wu, W., Wieckowski, S., Luangsivilay, J., Godefroy, S., Pantarotto, D., Briand, J.P., Muller, S., Prato, M., Bianco, A., 2007. Cellular uptake of functionalized carbon nanotubes is independent of functional group and cell type. Nature Nanotechnology 2 (2), 108–113.

Mitchell, D.N., Godwin, H.A., Claudio, E., 2004. Nonoparticle Toxicity in *Saccharomyces cerevisiae*: a comparative study using au colloid, Ag colloid, and $HAuCl4{\cdot}3H_2O$ in solution. Nanoscape 1, 59–69.

Navarro, E., Baun, A., Behra, R., Hartmann, N.B., Filser, J., Miao, A.-J., Quigg, A., Santschi, P.H., Sigg, L., 2008. Environmental behavior and ecotoxicity of engineered nanoparticles to algae, plants and fungi. Ecotoxicology 17, 372–386.

Ngoy, J.M., Iyuke, S.E., Neuse, W.E., Yah, C.S., 2011. Covalent functionalization for multi-walled carbon nanotube (*f-MWCNT*)-folic acid bound bioconjugate. Journal of Applied Sciences 11 (15), 2700–2711.

Pantarotto, D., Briand, J.P., Prato, M., Bianco, A., 2004. Translocation of bioactive peptides across cell membranes by carbon nanotubes. The Royal Society of Chemistry 1, 16–17.

Pastorin, G., Wu, W., Wieckowski, S., Briand, J.P., Kostarelos, K., Prato, M., Bianco, A., 2006. Double functionalisation of carbon nanotubes for multimodal drug delivery. Chemical communications 21 (11), 1182–1184.

Shvedova, A.A., Kisin, E.R., Porter, D., Schulte, P., Kagan, V.E., Fadeel, B., Castranova, V., 2009. Mechanisms of pulmonary toxicity and medical applications of carbon nanotubes: two faces of Janus? Pharmacology & Therapeutics 121 (2), 192–204.

Simate, G.S., Iyuke, S.E., Ndlovu, S., Yah, C.S., Walubita, L.F., 2010. The Production of carbon nanotubes from carbon dioxide – challenges and opportunities. Journal of Natural Gas Chemistry 19 (5), 453–460.

Warheit, D.B., Laurence, B.R., Reed, K.L., Roach, D.H., Reynolds, G.A., Webb, T.R., 2004. Comparative pulmonary toxicity assessment of single-wall carbon nanotubes in rats. Toxicological Sciences: An Official Journal of the Society of Toxicology 77 (1), 117–125.

Wu, X.Z., Chang, W.Q., Cheng, A.X., Sun, L.M., Lou, H.X., 2010. Plagiochin E, an antifungal active macrocyclic bis(bibenzyl), induced apoptosis in *Candida albicans* through a metacaspase-dependent apoptotic pathway. Biochimica et Biophysica Acta 1800 (4), 439–447.

Xu, Y., Wang, S.-Y., Yang, J., Gu, X., Zhang, J., Zheng, Y.-F., Yang, J., Xu, L., Zhu, X.-Q., 2011. Multiwall carbon nano-onions induced DNA damage and apoptosis in human umbilical vein endothelial cells. Environmental Toxicology. doi:10.1002/tox20736.

Yah, C.S., Simate, G.S., Moothi, K., Maphuta, S., 2011a. Synthesis of large carbon nanotubes from ferrocene: the chemical vapour deposition technique. Trends in Applied Sciences Research 6 (11), 1270–1279.

Yah, C.S., Iyuke, S.E., Simate, G.S., Unuabonah, E.I., Bathgate, G., Matthews, G., Cluett, J.D., 2011b. Continuous synthesis of multiwalled carbon nanotubes from xylene using the swirled floating catalyst chemical vapor deposition technique. Journal of Materials Research 26 (5), 623–632.

Zhou, F., Xiang, D., Wu, B., Wu, S., Ou, Z., Chen, W.R., 2010. New insights of transmembranal mechanism and subcellular localization of noncovalently modified single walled carbon nanotubes. Nano Letters, 1677–1681.